Journal of Hazardous Materials 160 (2008) 482–488

Contents lists available at ScienceDirect

Journal of Hazardous Materials

journal homepage: www.elsevier.com/locate/jhazmat

Hydrogen sulfide removal from coal gas by the metal-ferrite sorbents made from the heavy metal wastewater sludge

Ting Ke Tseng[a], Han Ching Chang[a], Hsin Chu[a,*], Hung Ta Chen[b]

[a] Department of Environmental Engineering and Sustainable Environment Research Center, National Cheng Kung University, 1 University Road, Tainan 701, Taiwan
[b] Sustainable Environment Research Center, National Cheng Kung University, Tainan, Taiwan

ARTICLE INFO

Article history:
Received 9 April 2007
Received in revised form 31 October 2007
Accepted 7 March 2008
Available online 20 March 2008

Keywords:
High temperature desulfidation
Chromium-ferrite
Zinc-ferrite
Heavy metal wastewater sludge
Coal gas
Hydrogen sulfide

ABSTRACT

The metal-ferrite (chromium-ferrite and zinc-ferrite) sorbents made from the heavy metal wastewater sludge have been developed for the hydrogen sulfide removal from coal gas. The high temperature absorption of hydrogen sulfide from coal gas with the metal-ferrite sorbent in a fixed bed reactor was conducted in this study. The metal-ferrite powders were the products of the ferrite process for the heavy metal wastewater treatment. The porosity analysis results show that the number of micropores of the sorbents after sulfidation and regeneration process decreases and the average pore size increases due to the acute endothermic and exothermic reactions during the sulfidation–regeneration process. The FeS, ZnS, and MnS peaks are observed on the sulfided sorbents, and the chromium extraction of the CFR6 can fulfill the emission standard of Taiwan EPA. The suitable sulfidation temperature range for chromium-ferrite sorbent is at 500–600 °C. In addition, effects of various concentrations of H_2 and CO were also conducted in the present work at different temperatures. By increasing the H_2 concentration, the sulfur sorption capacity of the sorbent decreases and an adverse result is observed in the case of increasing CO concentration. This can be explained via water-shift reaction.

1. Introduction

World primary energy demand increases with increases in population and economic development. Within the last 25 years, total energy consumption has almost doubled. In order to meet this demand, research into new sources of energy as well as improving the efficiency of energy production technologies is being carried out. In both cases, the production of clean energy is very important because of environmental concerns and regulations. Integrated gasification combined cycle (IGCC) processes are considered one of the most efficient and environmentally acceptable technologies for power generation from coal. For the use of these technologies, a highly efficient sulfur removal of the coal-derived fuel gas is needed. Hot gas desulfurization is a crucial issue in the development of the IGCC system [1].

The basic high temperature desulfidation reaction scheme can be presented as follows:

$$MO_{x(s)} + xH_2S_{(g)} \leftrightarrow MS_{x(s)} + xH_2O_{(g)} \quad (1)$$

where MO_x and MS_x are the metal oxide and metallic sulfide, respectively. The sulfide sorbent can regain the metal oxide by the regeneration process [2,3].

$$MS_{x(s)} + \tfrac{3x}{2}O_{2(g)} \leftrightarrow MO_{x(s)} + xSO_{2(g)} \quad (2)$$

Westmoreland and Harrison indicated that chromium metal was formed stable and unreactive oxide throughout the desulfurization temperature range (400–1200 °C) [4].

Iron oxide was the first metal oxide examined for hot gas desulfurization. The reactant phase is one of the stable forms of iron oxide (Fe_2O_3, Fe_3O_4, FeO or elemental Fe). Iron-based sorbents have been prepared from iron ores and reagent grade oxides combined with various binders or by loading on a support material. Among them, the most known type is zinc ferrite [5,6].

Zinc oxide has favorable thermodynamic properties and is capable of reducing the H_2S concentration in coal gas below 10 ppmv. However, in strongly reducing atmospheres and at temperatures above 650 °C, ZnO is reduced to metallic zinc and volatilized [7–9]. To prevent sorbent reduction, ZnO is combined with other metal oxides.

The first metal oxide mixed with ZnO was iron oxide forming zinc ferrite. Zinc oxide has a high equilibrium constant for sulfidation resulting in low equilibrium H_2S concentrations but has slow kinetics, which limits its sulfur loading capacity. Iron oxide, on the other hand, has rapid kinetics, namely a high sulfur loading capacity, but its equilibrium constant is not high enough for the degree of H_2S removal required in IGCC systems. It is also known that iron

* Corresponding author. Tel.: +886 6 208 0108; fax: +886 6 275 2790.
E-mail address: chuhsin@mail.ncku.edu.tw (H. Chu).

0304-3894/$ – see front matter © 2008 Elsevier B.V. All rights reserved.
doi:10.1016/j.jhazmat.2008.03.058

oxide is easily regenerable [7,8]. The purpose for zinc ferrite formation is to obtain a sorbent with superior thermodynamic properties (H_2S removal efficiency down to the ppmv level, high sulfur loading capacity and a high reactivity) [7].

Among the sludge produced, precipitated ferrites are generated in the ferrite process. Ferrite process was used to treat chromium, copper, nickel and zinc in the electroplate wastewater. Ferrites, which may be expressed as $M_xFe_{3-x}O_4$ where M may be Ni, Mn, Mg, Zn, Cu or Cr are ferromagnetic materials [10–12]. The ferrite precipitate is composed mainly of magnetite which undergoes partial isomorphic substitution of Fe^{3+} or Fe^{2+} ions by the metal ions initially present in the wastewater [13].

There are three important factors for the best conditions in the metal-containing wastewater purification, such as pH (9–12), $[Fe^{2+}]/[M^{n+}]$ molar ratio (4–20) and temperature (60–80 °C) were investigated [14–16]. The reaction is shown as below [14]

$$3FeSO_4 + 6NaOH + \tfrac{1}{2}O_2 \rightarrow Fe_3O_4 + 3Na_2SO_4 + 3H_2O \quad (3)$$

Metal (M^{n+}) will occupy the positions of some Fe^{2+} and Fe^{3+} in the magnetite structure. The reaction is shown in Eq. (4) below [14]

$$xM^{n+} + 3FeSO_4 + 6NaOH + \tfrac{1}{2}O_2 \rightarrow M_xFe_{3-x}O_4 + 3Na_2SO_4 + 3H_2O + xFe^{n+} \quad (4)$$

The objects of the present work are the feasibility of H_2S removal on the metal-ferrite sorbent and try to indicate the crystal phase change of the metal-ferrite sorbent from the H_2S removal process.

2. Experimental

2.1. Sorbents preparation

The metal-ferrite powders were the products of the ferrite process for the heavy metal wastewater treatment. The wastewater containing various heavy metals $[Cr^{2+}] = 600$ ppm of chromium series wastewater and $[Zn^{2+}] = 600$ ppm of zinc series wastewater, respectively, were obtained from one electroplating plant in Taiwan. Many apparatus were used in this experiment, such as: pH meter, ORP meter, oven, heater, vacuum filtration apparatus, filter paper and thermal control meter. The heavy metal wastewater of the electroplating plant were mixed with a $[Fe^{2+}/M^{n+}]$ molar ratio of 8:1 in an 80 L tank. When mixed thoroughly, a digital pH meter was used to monitor the pH of wastewater. It was adjusted at pH 10.5 by adding 1N sodium hydroxide solution. The content of the tank was heated at 70 °C by an electric furnace. At the same time, the wastewater was aerated (the aeration rate was 80 L min^{-1}) and its oxidation–reduction potentials (ORP) was detected by using ORP

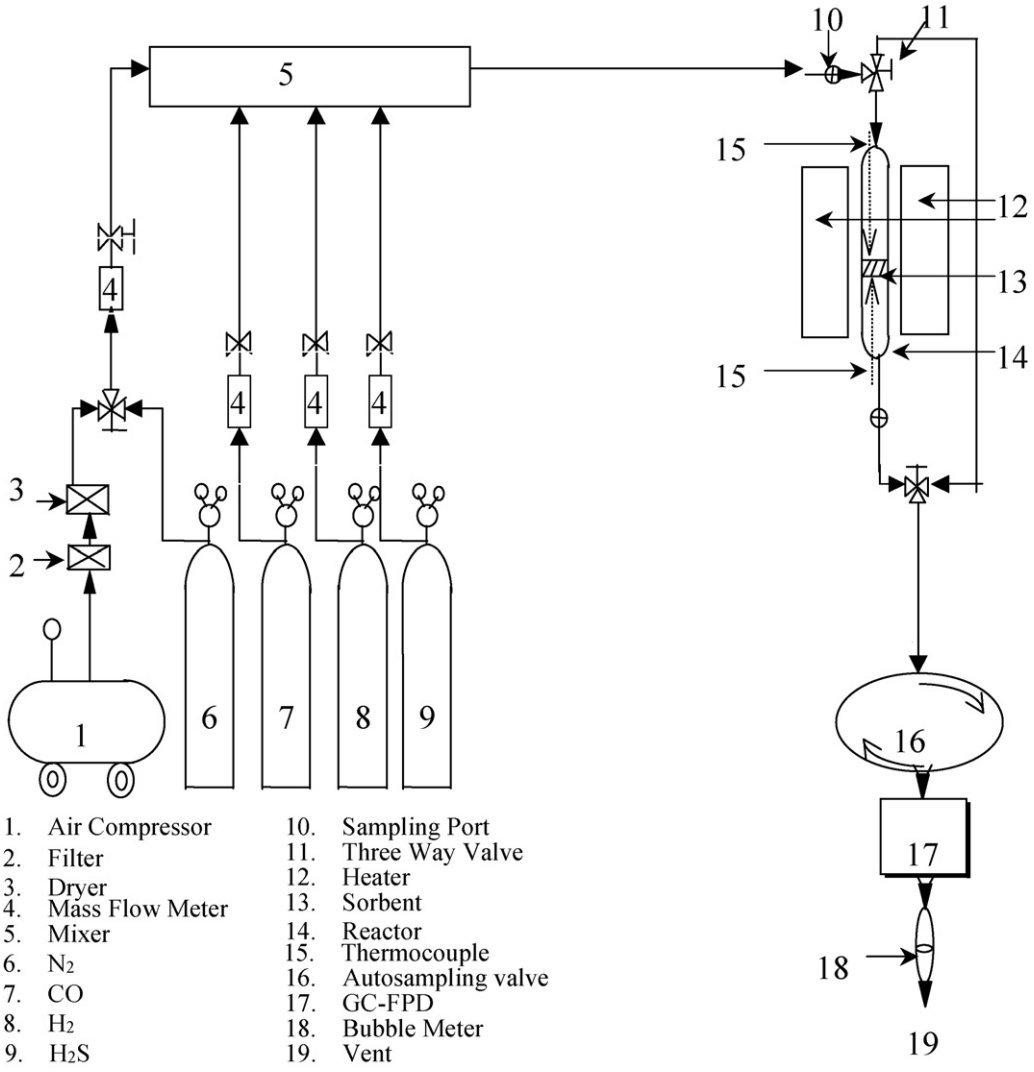

Fig. 1. A schematic diagram of the lab-scale experimental system.

meter. Finally, the precipitate formed was separated from the liquid phase by a vacuum filtration apparatus and put into the oven at 105 °C for 4 h.

N-150 sorbent supplied by NISSAN GIRDLER Company, Japan, was also used in this study, which contained about 30% MnO and 60% Fe_2O_3 and 10% inert material.

The sorbent labels used in this study were defined as follows: fresh chromium-ferrite (CF), chromium-ferrite sulfide at 500 °C (CF5), chromium-ferrite sulfide at 600 °C (CF6), fresh zinc-ferrite (ZF), zinc-ferrite sulfide at 500 °C (ZF5), zinc-ferrite sulfide at 600 °C (ZF6), fresh N-150 sorbent (N-MF), N-150 sulfide at 600 °C (N-MF6), chromium-ferrite sulfide at 500 °C and regenerated three times (CF5R3), chromium-ferrite sulfide at 500 °C and regenerated five times (CF5R5).

2.2. Sorbents characterization

The sorbents' surface areas and average pore diameters were measured through N_2 adsorption at liquid-nitrogen temperature by a surface area analyzer (Micromeritics ASAP 2400).

The DTA–TGA (differential thermal analysis–thermogravimetric analysis) analysis was carried out in 4.7% H_2 in He (100 mL min^{-1}) on a thermogravimetric analyzer (Pyris Diamond TG/DTA, PerkinElmer instruments); the temperature cycle was programmed from 40 to 1100 °C at a rate of 10 °C min^{-1}.

An X-ray diffractometer (Rigaku D/max III V XRD) was used to analyze the catalysts' structures. The radiation source was Cu Kα. The applied current and voltage were 30 mA and 40 kV, respectively. During the analysis, the sample was scanned from 10° to 80° at a speed of 0.4° min^{-1}.

Concentrations of the metal oxides were determined by inductively coupled plasma (ICP). After the digestion, filtration and dilution processes, the extracted solution was analyzed by inductively coupled plasma atomic emission spectrometry (ICP/AES, JY38P model, JOBIN YVON).

Elementar vario EL III Heraeus CHNOS Rapid F002, equipped with a flash combustion furnace and thermal conductivity detector (TCD), was used for carbon and sulfur determination.

2.3. Sorption experiments

The sulfidation experiment mainly consisted of three sections and shown in Fig. 1: (1) a coal gas simulation system; (2) a desulfidation reaction system; and (3) an effluent gas analyzing system. The composition of major simulation coal gases were composed of 1% H_2S, 25% CO, 15% H_2, and 59% N_2, which were similar to the quenched exit gas of the popular KRW coal gasifier. Gases were supplied from gas cylinders and flow rates were monitored through mass flow controllers. Prior to their use, the gases were conducted into a mixing pipe to confirm that mixture gases were in turbulence.

The desulfidation of this study was conducted in a bench scale fixed bed reactor under atmospheric pressure. It consisted of a 1.5 cm i.d., 1.8 cm o.d., and 85 cm length quartz tube located inside an electrical furnace. A frit quartz disk was set in the reactor, 45 cm below the top of the tube, to support the sorbent. The weight of sorbent packing was 1.5 g (thickness 0.85 cm). The temperature was monitored by a K-type thermocouple to the reactor so that its tip was exactly at the top of the sorbent bed and controlled by a TTE TM-4800 temperature controller. Blank breakthrough experiments were conducted at the reaction conditions and confirmed that no sorption/reaction of H_2S was taking place anywhere along the lines.

The inlet and outlet H_2S concentration analysis were conducted on-line with a gas chromatograph (Shimadzu, GC-14B) equipped with a flame photometry detector (FPD) and fitted with a GS-Q capillary column. The inlet and outlet gas stream was sampled every 3 min in all cases.

The sulfidation test was conducted at 500 and 600 °C, respectively, with 1% H_2S mixture gas and the weight hourly space velocity (WHSV) was controlled at 4000 mL h^{-1} g^{-1}. The breakthrough point was defined as the time of the H_2S concentration reach to 100 ppm and then abrupt change in the exit gas. After the sulfidation test, the reactor was purged with nitrogen gas for 15 min, and then regeneration was begun at 500 and 600 °C, respectively, with 5% O_2 under the same weight hourly space velocity, 4000 mL h^{-1} g^{-1}.

3. Results and discussions

3.1. Sorbent preparation

The experiments were divided into three parts. The first part was conducted to investigate the performance of the three sorbents on H_2S removal. The second part was performed to study the effect of reaction temperature (25–700 °C) on H_2S removal from coal gas. A simulated reduction reaction of the zinc-ferrite sorbent by using the TPR technique was also conducted to identify the temperature limitation. The third part was performed to study the effect of CO concentration (0 and 25%) and H_2 concentration (0 and 15%) on H_2S removal.

The basic properties and element analysis of the three and five times regeneration of chromium-ferrite were performed and shown in Table 1 and Fig. 2. As shown in Table 1, the surface area and the pore volume of sorbents was extremely low after the desulfidation process. These may be due to the fact that the sulfur penetrates into the crystal of the sorbents to substitute oxygen. This is consistent with the result of element analysis shown in Table 1 that the sulfur contents on the sulfided sorbents are large than that of the fresh sorbents. As shown in Fig. 2, the pore volumes of fresh CF sorbent are 0.035 and 0.028 cm^3 g^{-1} at median pore sizes of 44.1 and 94.3 nm, respectively, while those of the CF5, CF5R3 and CF5R5 sorbents are 0.0083, 0.0142, and 0.0118 cm^3 g^{-1} at median pore sizes of

Table 1
Basic properties and element analysis of various sorbents

Sorbent	BET surface area (m^2 g^{-1})	Total pore volume (cm^3 g^{-1})	Average pore diameter (nm)	Carbon (%)	Sulfur (%)
CF	104	0.16	6.2	0.26	0.43
CF5	17	0.04	8.6	6.82	20.94
CF6	21	0.07	14.0	2.49	21.89
ZF	555	1.97	14.2	0.21	1.69
ZF5	38	0.05	4.7	17.63	23.99
ZF6	31	0.04	4.8	5.70	25.96
N-MF	129	0.23	69.8	1.65	1.25
N-MF6	–	–	–	3.72	22.28
CF5R3	8	0.03	14	–	0.79
CF5R5	6	0.02	14	–	1.47

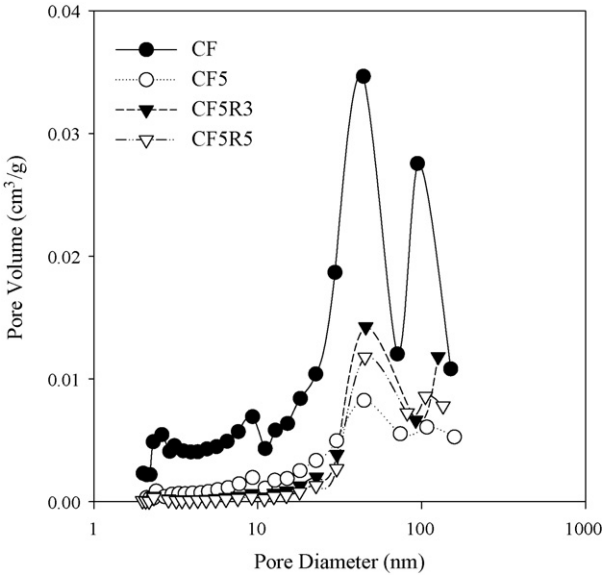

Fig. 2. Pore diameter distributions for the Cr-ferrite.

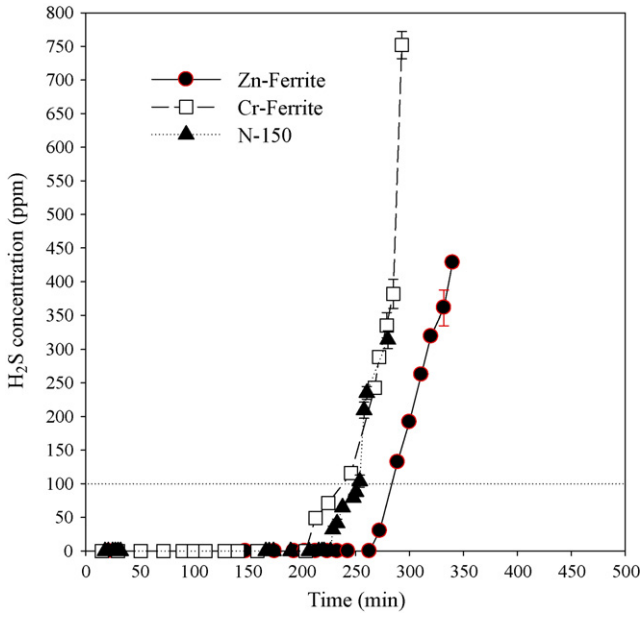

Fig. 3. Breakthrough curve of H_2S removal on the various sorbents, C_{H_2S} = 1%, C_{CO} = 25%, C_{H_2} = 15%, with balance N_2.

44.5, 45.7, and 45.1 nm, respectively. These results mean that the CF sorbent has a number of median pore sizes, and the CF5, CF5R3 and CF5R5 have one median pore size after sulfidation and regeneration process. This may be due to the acute endothermic and exothermic reaction during the sulfidation–regeneration process, making the micropore (less than 10 nm) sintering. Therefore, the number of micropore decreases and the average pore size increases.

3.2. Sorbents characterization

Table 2 shows the inductively coupled plasma (ICP) analysis for various sorbents. The results indicate that the element mass percentages of the fresh sorbents are Fe (62.3%), Cr (4%) for CF; Fe (68.1%), Zn (7%) for ZF; and Fe (37.8%), Mn (22.2%) for N-MF. The sulfidation reactions of various sorbents are expressed as below:

$$\text{chromium-ferrite}: \quad Fe_3O_4 + 3H_2S + H_2 \leftrightarrow 3FeS + 4H_2O \quad (5)$$

$$\text{zinc-ferrite}: \quad ZnFe_2O_4 + 3H_2S + H_2 \leftrightarrow ZnS + 2FeS + 4H_2O \quad (6)$$

$$\text{N-150}: \quad Fe_2O_3 + 2H_2S + H_2 \leftrightarrow 2FeS + 3H_2O \quad (7)$$

$$MnOOH + H_2S + \tfrac{1}{2}H_2 \leftrightarrow MnS + 2H_2O \quad (8)$$

According to the results of the element mass percentage, the theoretical sulfur capacity (TSC) can be calculated through the possible sulfidation reactions (reactions (5)–(8)). As shown in Table 2, column of sorption capacity, the TSC values of the three sorbents are 35.7 g-S/100 g-sorbent for CF, 42.3 g-S/100 g-sorbent for ZF, and 34.5 g-S/100 g-sorbent for N-MF, respectively.

In order to compare the desulfidation property of various sorbents, the sulfur capacity (SC) was also used. The definition of the sulfur capacity was defined as follows:

$$SC\left(\frac{\text{g-sulfur}}{100\,\text{g-sorbent}}\right) = (\text{WHSV}) \times \left[\frac{M}{24.5} \times \int_0^t (C_{in} - C_{out})\,dt\right] \quad (9)$$

where WHSV is the weight hourly space velocity (mL h^{-1} g^{-1}), M is the molecular weight of H_2S, the mole volume of H_2S at 25 °C, 1 atm, is 24.5 L mol^{-1}, C_{in} and C_{out} are the H_2S inlet and outlet concentrations (%), respectively, and t is the breakthrough time of desulfidation process (min).

Fig. 3 shows the breakthrough curves of H_2S removal on the three sorbents, such as chromium-ferrite, zinc-ferrite, and N-150 sorbent. As shown in Fig. 3, the time of breakthrough point for the three sorbents are 282 min for ZF6, 252 min for N-MF6, and 239 min for CF6, respectively.

According to Eq. (9), the calculated sulfur capacity (CSC) can be addressed by giving the WHSV = 4000 mL h^{-1} g^{-1}, C_{in} = 1% = 10,000 ppm, C_{out} = 0.01% = 100 ppm, and the breakthrough time of the three sorbents with CF6 = 239 min, N-MF6 = 252 min, and ZF6 = 282 min, respectively. The results show that the CSC value (26.1 g-S/100 g-sorbent) of zinc-ferrite is the highest among them because the zinc-ferrite has the highest iron mass percentage. The CSC values of various sorbents also consist with the results of the element analysis, as shown in Table 1, it indicates that Eq. (9) can exactly calculate the sulfur capacity from the desulfidation reaction.

The sorbent utilization (SU) of various sorbents can also be defined as Eq. (10) and the results shown in Table 2.

$$SU(\%) = \frac{CSC}{TSC} \times 100\% = \frac{t}{t_0} \times 100\% \quad (10)$$

where t_0 is the theoretical breakthrough time (min), calculated by substituting TSC into Eq. (9).

The results indicate that the N-150 commercial sorbent has the highest sorbent utilization among them, however, it is not good enough to reach 100%.

Fig. 4 shows the X-ray diffraction spectra of various sorbents. The principal peaks at 2θ = 30.08°, 35.43°, 43.05°, 53.41°, 56.94°, and 62.52° in the spectra of CF and ZF do not appear in the spectrum of CF6 and ZF6. According to the Joint Committee on Powder

Table 2
ICP analysis and sorption capacity for the sorbents at various status

Sorbents	Element mass percentage (%)				Sorption capacity (%)		
	Fe	Cr	Zn	Mn	TSC	CSC	SU (%)
CF	62.3	4.0	ND	ND	35.7		
CF6						22.2	62.2
ZF	68.1	ND	7.0	ND	42.3		
ZF6						26.1	61.7
N-MF	37.8	ND	ND	22.2	34.8		
N-MF6						23.4	67.2

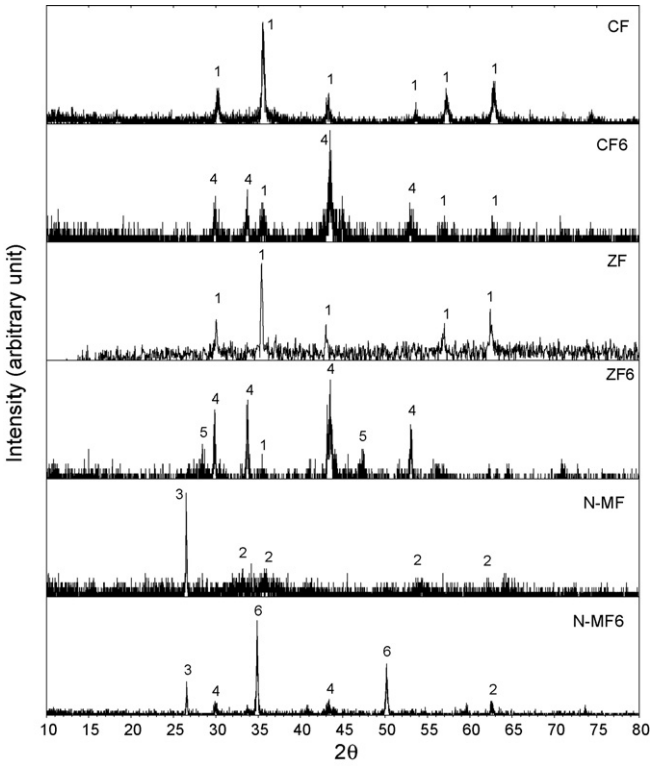

Fig. 4. XRD spectra of the fresh and sulfided at 600 °C sorbents. (1) Fe_3O_4, (2) Fe_2O_3, (3) MnOOH, (4) FeS, (5) ZnS, and (6) MnS.

Diffraction System (JCPDS) file, the principal peaks represent Fe_3O_4 [82-1533]. The principal peaks at $2\theta = 29.84°$, 33.59°, 43.14°, and 52.97° in the spectra of CF6 and ZF6 represent the iron sulfide crystal phase. According to the JCPDS file, the principal peaks represent FeS [80-1027]. The peaks of $CrFe_2O_4$ and $ZnFe_2O_4$ are not observed in the spectra of CF and ZF, since the peak positions of the $CrFe_2O_4$ and $ZnFe_2O_4$ are similar to the peaks of Fe_3O_4. Besides iron sulfide peaks, poor crystal phase is found on ZnS [05-0492] at $2\theta = 28.51°$ and 47.54° in the spectrum of ZF6.

The result suggests that the main crystal phase of the sulfided sorbent is FeS. There are small Fe_3O_4 peaks appearing in the spectra of CF6 and Zf6. This can be the evidence for the bad sorbent utilization of the M-ferrite sorbents.

For the spectrum of N-MF, an intense peak is observed around $2\theta = 26.38°$. According to the JCPDS file, the principal peak represents MnOOH [74-1842] is a strong crystalline structure. Poor crystal phase is detected at $2\theta = 32.21°$, 35.73°, 54.17°, and 62.68° for Fe_2O_3 [85-0987]. The absence of intense XRD spectra for iron oxides indicates that iron oxides may be presented in a highly dispersed amorphous state.

After sulfidation test at 600 °C, the peaks at $2\theta = 34.20°$ and 49.14° in the spectrum of N-MF6 do not appear in the spectrum of N-MF. According to the JCPDS file, the peaks represent MnS [75-1543]. The FeS peaks are also observed in the spectrum of N-MF6. In addition, there are small peaks representing Fe_2O_3 crystal phase appearing in the spectrum of N-MF6. This suggests that the metal oxides of the fresh sorbent did not completely convert into metal sulfides in the sulfided sorbents and it consist with the result of the sorbent utilization shown in Table 2. It may be due to that the metal sulfides are dense materials, which will increase the mass transfer resistance and retard H_2S diffusing into the core of sorbents.

Table 3 shows the results of toxic characteristic leaching procedure (TCLP) test of the fresh, sulfided and regenerated chromium-ferrite sorbents. As shown in Table 3, the chromium extraction of the sulfided sorbent cannot comply the emission standard of Taiwan EPA. Nevertheless, after regenerating process, there is no chromium extraction detected in the regenerated sorbent. From this observation, we infer that major part of metal sulfides is converted to the metal oxides after the 500 °C regeneration process.

Table 3
TCLP test of the fresh, sulfided and regenerated Cr-ferrite

Sorbent	Extraction value of chromium (mg L^{-1})
CF	0.13
CF5	15
CFR5	ND
Emission standard of Taiwan EPA	5

3.3. Sorption experiments

3.3.1. Effect of sulfidation temperature

A series of experiments with sulfidation temperatures from 25 to 700 °C were conducted in this study to examine the effect of sulfidation temperature on the metal-ferrite sorbents in a bench scale fixed bed reactor. Fig. 5 presents the breakthrough curves as a function of sorbent utilization for the chromium-ferrite evaluated in this study. As shown in this figure, the sorbent utilization, as well as the breakthrough time, decreases as the sulfidation temperature increases from 500 to 700 °C. The sulfided sorbent at 600 °C has almost the same sorbent utilization compared with the sulfided sorbent at 500 °C as shown in H_2S breakthrough curves in Fig. 5, which indicates that the suitable sulfidation temperature range for chromium-ferrite sorbent is at 500–600 °C. This is consistent with the results obtained by a previous study [17], which the results showed that breakthrough time of the Fe_2O_3 sorbent decreased from 32 to 15 min as the temperature increased from 600 to 750 °C.

As shown in Fig. 5, high temperature detrimentally affected the removal of H_2S from coal gas. In order to realize the temperature limitation of H_2S removal, a simulated reduction reaction was conducted in this study. The simulated reduction gas consist of 4.7% H_2 balanced in He at a heating rate of 10 °C min^{-1} for the zinc-ferrite sorbent in a TG–DTA analyzer. This is also called temperature

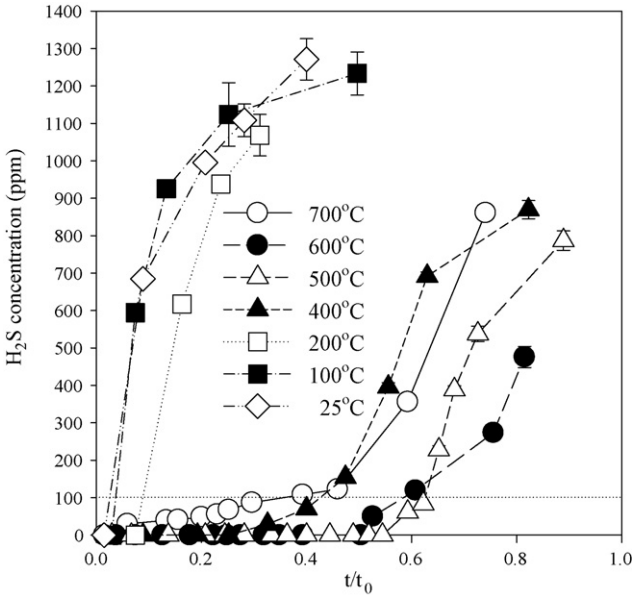

Fig. 5. Breakthrough curve of H_2S removal on the Cr-ferrite at various temperatures, $C_{H_2S} = 1\%$, $C_{CO} = 25\%$, $C_{H_2} = 15\%$, with balance N_2.

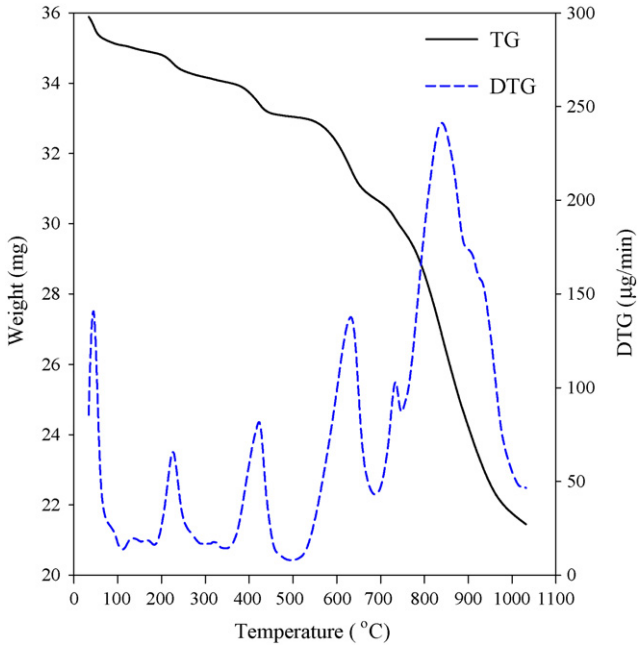

Fig. 6. TPR profiles for the zinc-ferrite sorbent.

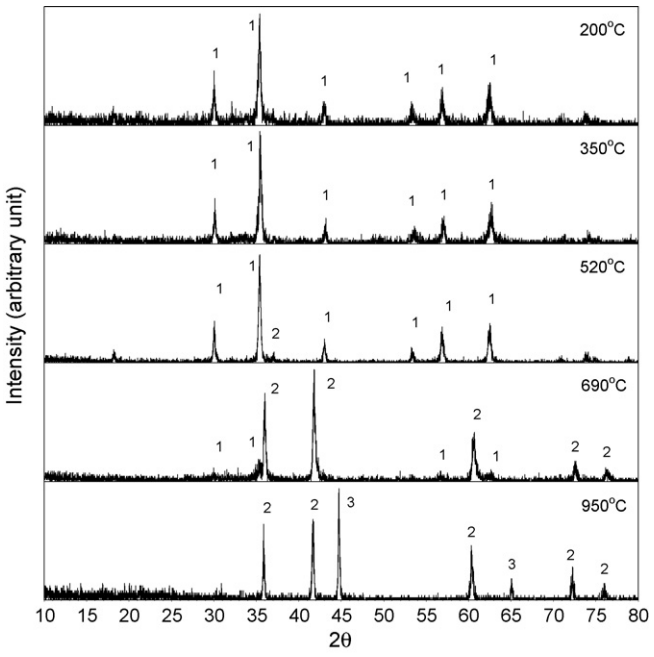

Fig. 7. XRD spectra of zinc-ferrite sorbent at various temperatures during the TPR process: (1) Fe_3O_4, (2) FeO, and (3) Fe.

programming reduction (TPR) technique. The results of TG–DTA analysis is shown in Fig. 6. From this figure, the TGA curve indicates that the weight of zinc-ferrite sorbent declines from 36 to 21 mg, and that five principal peaks at 50, 225, 420, 630, and 850 °C appear in the DTG curve. The results suggest that the weight loss phenomena might be due to the loss of moisture adsorbed on zinc-ferrite sorbent and the loss of metal salt that added in the sorbent preparation process at 50 and 225 °C, respectively. In order to realize the crystal changes of the zinc-ferrite sorbent for the other three weight loss peaks at 420, 630, and 850 °C, respectively. The zinc-ferrite sorbent was taken out at the bottom temperature after each peak temperature for the X-ray diffraction analysis and the results are shown in Fig. 7.

As shown in Fig. 7, the principal peaks represent Fe_3O_4 crystal phase in the spectrum of 200, 350, and 520 °C reduction temperature do not appear in the spectrum of reduction temperature 690 and 950 °C, and the peak intensity of the 350 °C reduction temperature is higher than those for the 200 and 520 °C reduction temperatures. The result indicates that the main crystal phase in Fe_3O_4 does not change at the 200, 350, and 520 °C reduction temperatures. There is a small peak at $2\theta = 36.20°$, according to JCPDS file, representing FeO, appearing in the spectrum of 520 °C reduction temperature. This phenomenon suggests that the absence of intense XRD spectra in FeO indicates that the FeO crystal phase may present in a highly dispersed amorphous state during the reduction temperature range from 350 to 520 °C.

For the reduction temperature 690 °C, the principal peaks at $2\theta = 36.20°$, 42.05°, 60.98°, 73.02°, and 76.84° are observed and these do not appear in the spectrum of the lower reduction temperature state. The result indicates that the major part of Fe_3O_4 of the 520 °C reduction temperature state is converted to FeO after the 630 °C reducing process. The principal peaks at $2\theta = 44.67°$ and 65.02° in the spectrum of 950 °C reduction temperature do not appear in the spectrum of 690 °C reduction temperature. According to the JCPDS file, the principal peaks represent Fe [06-0696]. This indicates that the FeO crystal phase of the 690 °C reduction temperature is reduced to the Fe crystal phase in a reduction atmosphere.

According to Fig. 6, the results prove that the weight loss phenomenon may be due to the Fe_3O_4, FeO, and Fe crystal changes at 420, 630, and 850 °C, respectively. As the results of TG–DTG and XRD spectra shown in Figs. 6 and 7, respectively, such a phase change (Fe_3O_4–FeO–Fe) has been found in this study. Corresponding to the results shown in Fig. 5, the iron oxides have high sulfur sorption capacity and are highly reactive with H_2S. A high temperature (700 °C) detrimentally affects the reaction of H_2S removal due to the reduction of Fe_3O_4 to FeO or Fe in a reduction atmosphere. The FeO has been shown to be an unfavorable sorbent for H_2S [18,19]. This phenomenon also can be explained through thermodynamic properties. The sulfidation reactions of Fe_3O_4 and FeO are expressed as Eq. (5) and follows:

$$FeO + H_2S \rightarrow FeS + H_2O \quad (11)$$

The equilibrium constants of Fe_3O_4 and FeO at 500, 600, and 700 °C, respectively, were conducted and the results indicated that the sulfidation equilibriums of Fe_3O_4 are vastly superior to that of FeO. In a reduction atmosphere, the iron oxides in zinc-ferrite sorbents initially suffer reduction and the desulfidation reaction follows. Therefore, if the temperature exceeds 600 °C, Fe_3O_4 will be reduced to FeO, an unfavorable sorbent for H_2S.

As shown in Fig. 5, the adequate range of temperatures for the desulfidation reaction by chromium-ferrite is 500–600 °C. The recent studies have revealed that the desulfidation system components become prohibitively expensive as the operating temperature increases and the optimum desulfidation temperature is between 350 and 650 °C [20]. To overtake the temperature range, the efficiency of the process and its technical viability reduce the overall cost of the process. Additionally, many sorbents can reduce the concentration of H_2S below the maximum tolerable level (less than 10 ppm) because the thermodynamic equilibrium is favorable from 350 to 650 °C. These findings are supporting that chromium-ferrite and zinc-ferrite can be developed as a suitable sorbent for H_2S.

3.3.2. *Effect of CO and H_2 concentrations*

Besides hydrogen sulfide, carbon monoxide and hydrogen are the main products of coal gasification and influence the desul-

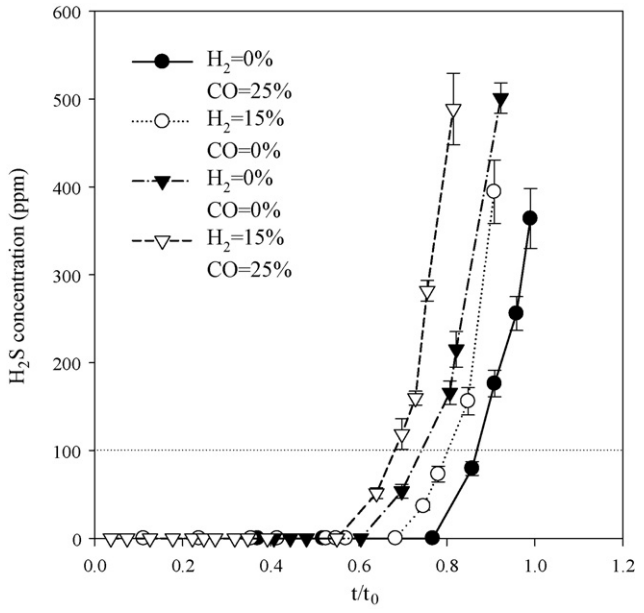

Fig. 8. Effect of carbon monoxide and hydrogen of H_2S removal on the Cr-ferrite at 500 °C, $C_{H_2S} = 1\%$, $C_{CO} = 0$ and 25%, $C_{H_2} = 0$ and 15%, with balance N_2.

fidation reaction critically. Fig. 8 shows the influence of carbon monoxide and hydrogen on the breakthrough curve of chromium-ferrite sulfided at 600 °C. The inlet gas consists of 1% H_2S, various concentration of CO (0–25%) and H_2 (0–15%), and balanced in N_2. As shown in Fig. 8, the breakthrough points depend on the concentrations of carbon monoxide and hydrogen. The results indicate that carbon monoxide has a positive effect and hydrogen has an opposite effect for the H_2S removal on the chromium-ferrite sorbent at 600 °C. These positive and negative effects can be explained by the water-shift reaction and reaction (5):

$$\text{Water-shift reaction}: \quad CO + H_2O \leftrightarrow H_2 + CO_2 \tag{12}$$

As the concentration of carbon monoxide increase, according to the LeChatelier's principle the water-shift reaction favors toward the right side, indicating that H_2O is consumed via water-shift reaction. A lower H_2O content will promote the desulfidation reaction, therefore, increasing the concentration of carbon monoxide enhances desulfidation. On the other hand, increasing the concentration of hydrogen favors to the left side of the water-shift reaction, resulting in the formation of H_2O. The progress of desulfidation is, therefore, inhibited by the formation of excess H_2O.

4. Conclusions

The present work deals with hydrogen sulfide from coal gas by means of the chromium-ferrite and zinc-ferrite sorbents, which were tested in a fixed bed reactor. The metal-ferrite powders were prepared by the ferrite process for the heavy metal wastewater treatment. The porosity analysis results show that the surface area and the pore volume are extremely low for the desulfidation process. The XRD scan shows that the FeS, ZnS, and MnS peaks are observed on the sulfided sorbents. TCLP test results indicate the chromium extraction of the CFR6 can comply the emission standard of Taiwan EPA. The results of the performance test show that the time of breakthrough point for the three sorbents are 282 min for ZF6, 252 min for N-MF6, and 239 min for CF6, respectively.

A simulated reduction reaction was conducted in this study to realize the temperature limitation of H_2S removal. As the results of TG–DTG and XRD spectra shown, respectively, such a phase change (Fe_3O_4–FeO–Fe) has been found. Corresponding to the results of the H_2S removal on the chromium-ferrite at various temperatures, the iron oxides have high sulfur sorption capacity and are highly reactive with H_2S. A high temperature (700 °C) detrimentally affects the reaction of H_2S removal due to the reduction of Fe_3O_4 to FeO or Fe in a reduction atmosphere. The FeO has been shown to be an unfavorable sorbent for H_2S.

The suitable sulfidation temperature range for chromium-ferrite sorbent is at 500–600 °C. In addition, effects of various concentrations of H_2 and CO were also conducted in the present work at different temperatures. By increasing the H_2 concentration, the sulfur sorption capacity of the sorbent decreases and an adverse result is observed in the case of increasing CO concentration. This can be explained via water-shift reaction.

Acknowledgement

This study was funded in part by the Ministry of Economic Affairs of Republic of China (92-EC-17-A-10-S1-007).

References

[1] A.T. Atimtay, Cleaner energy production with integrated gasification combined cycle systems and use of metal oxide sorbents for H_2S cleanup from coal gas, Clean Prod. Pro. 2 (2001) 197–208.
[2] N. Park, D.C. Han, G.B. Han, S.O. Ryu, T.J. Lee, K.J. Yoon, Development and reactivity tests of Ce–Zr-based Claus catalysts for coal gas cleanup, Fuel 86 (2007) 2232–2240.
[3] S.C. Christoforou, E.A. Efthimiadis, I.A. Vasalos, Sulfidation of mixed metal oxides in a fluidized-bed reactor, Ind. Eng. Chem. Res. 34 (1995) 83–93.
[4] P.R. Westmoreland, D.P. Harrison, Evaluation of candidate solids for high-temperature desulfurization of low-BTU gases, Environ. Sci. Technol. 10 (1976) 659–661.
[5] S. Lew, K. Jothimurugesan, M.F. Stephanopoulos, High-temperature H_2S removal from fuel gases by regenerable zinc oxides-titanium dioxide sorbent, Ind. Eng. Chem. Res. 28 (1989) 535–541.
[6] E. Sasaoka, M. Sakamoto, T. Ichio, S. Kasaoka, Y. Sakata, Reactivity and durability of iron oxide high temperature desulfurization sorbents, Energy Fuels 7 (1993) 632–638.
[7] R.E. Ayala, D.W. Marsh, Characterization and long-range reactivity of zinc ferrite in high-temperature desulfurization processed, Ind. Eng. Chem. Res. 30 (1991) 55–60.
[8] E. Garcýía, C. Cilleruelo, J.V. Ibarra, M. Pineda, J.M. Palacios, Kinetic study of high-temperature removal of H_2S by novel metal oxide sorbents, Ind. Eng. Chem. Res. 36 (1997) 846–853.
[9] N. Ikenaga, Y. Ohgaito, H. Matsushima, T. Suzuki, Preparation of zinc ferrite in the presence of carbon material and its application to hot-gas cleaning, Fuel 83 (2004) 661–669.
[10] C.J. Smithells, E.A. Brandes, Metals Reference Book 5th, Butterworths, London, 1976.
[11] B. Demirel, O. Yenigun, M. Bekbolet, Removal of Cu, Ni and Zn from wastewaters by the ferrite process, Environ. Technol. 20 (1999) 963–970.
[12] R.S. Carmichael, Practical Handbook of Physical Properties of Rocks and Minerals, CRC, Boca Raton, FL, 1989.
[13] E. Barrado, M. Vega, R. Pardo, P. Grande, J. Valle, Optimisation of a purification method for metal-containing wastewater by use of a Taguchi experimental design, Water Res. 30 (1996) 2309–2314.
[14] E. Barrado, F. Prieto, M. Vega, F. Fernandez-Polanco, Optimization of the operational variables of a medium scale reactor for metal containing wastewater purification by ferrite formation, Water Res. 32 (1998) 2061–3055.
[15] Y. Tamaura, T. Katsura, S. Rojarayanont, T. Yoshida, H. Abe, Ferrite process; heavy metal ions treatment system, Water Sci. Technol. 23 (1991) 1893–1900.
[16] M.M. Benjamin, K.F. Hayes, J.O. Leckie, Removal of toxic metals from power generation waste streams by adsorption and coprecipitation, J. Water Pollut. Control Fed. 54 (1982) 1472–1481.
[17] M. Yumura, E. Furimsky, Comparison of CaO, ZnO and Fe_2O_3 as H_2S adsorbents at high temperatures, Ind. Eng. Chem. Process. Des. Dev. 24 (1985) 1165–1168.
[18] G.D. Focht, P.V. Ranade, D.P. Harrison, High temperature desulfurization using zinc ferrite: reduction and sulfidation kinetics, Chem. Eng. Sci. 43 (1988) 3005–3013.
[19] R.P. Gupta, S.K. Gangwal, S.C. Jain, Development of zinc ferrite sorbents for desulfurization of hot coal gas in a fluid-bed reactor, Energy Fuels 2 (1992) 21–27.
[20] R.B. Slimane, J. Abbasian, Regenerable mixed metal oxide sorbents for coal gas desulfurization at moderate temperature, Adv. Environ. Res. 4 (2000) 147–162.